Available online at www.sciencedirect.com
ScienceDirect
Journal of Organometallic Chemistry 692 (2007) 3882–3891
Journal of Organometallic Chemistry
www.elsevier.com/locate/jorganchem

About the different reactivity of dinuclear palladium and platinum compounds with trispyrrolylphosphine: Synthesis and X-ray crystallographic results of new palladium complexes containing P–pyrrolyl bonds

Inma Angurell [a], Isabel Martínez-Ruiz [a], Oriol Rossell [a], Miquel Seco [a,*], Pilar Gómez-Sal [b], Avelino Martín [b], Mercé Font-Bardia [c], Xavier Solans [c]

[a] Departament de Química Inorgànica, Universitat de Barcelona, Martí i Franquès 1-11, E-08028 Barcelona, Spain
[b] Departamento de Química Inorgánica, Universidad de Alcalá, E-28071 Alcalá de Henares, Spain
[c] Departament de Cristal·lografia, Mineralogia i Dipòsits Minerals, Universitat de Barcelona, Martí i Franquès s/n, 08028 Barcelona, Spain

Received 4 May 2007; received in revised form 21 May 2007; accepted 21 May 2007
Available online 2 June 2007

Abstract

The reaction of $[Pt(\mu\text{-}Cl)(\kappa,\eta^2\text{-}COE\text{-}MeO)]_2$ (**2**) (COE-MeO = 2-methoxy-5-cycloocten-1-yl) with trispyrrolylphosphine yields $[PtCl\{P(pyrl)_3\}(\kappa,\eta^2\text{-}COE\text{-}MeO)]$ (**3**), in contrast to the crown-cycle complex $[Pd(\mu\text{-}Cl)\{P(pyrl)_3\}]_8$ (**1**) obtained with the analogous palladium complex. The different reactivity has been explained in terms of the higher lability of the carbon–carbon double bond in the starting palladium compound, as compared with the related platinum derivative. The reaction of **1** with the ligand 2-[(pyridin-2-ylmethylene)aminophenol], (HNN′O), in the presence of thalium salt and NEt_3, yields the complex $[Pd(\kappa^3N,N',O\text{-py-CH=N-}C_6H_4O)(P(O)(pyrl)_2)]$ (**5**), which contains, for the first time, a di(*N*-pyrrolyl)phosphonato-*P* ligand. Treatment of $[PdCl(\kappa^3N,N',O\text{-py-CH=N-}C_6H_4O)]$ with $P(pyrl)_3$ gives the amido derivative $[PdCl\{\kappa^3P,N,N\text{-}(P(pyrl)_2\text{-O-}C_6H_4\text{-N-CH}(CH_2\text{-CO-}CH_3)\text{-py})\}]$ (**7**), which displays a N–Pd–P–O–C_2 six-membered metallacycle. In addition, the latter compound has been able to insert an acetone molecule into its framework. The crystal structures of **5** and **7** were solved by X-ray diffraction analysis.

Keywords: Palladium complexes; Trispyrrolylphosphine; Imine; Phosphonate; Insertion

1. Introduction

There is ongoing interest in the study of *N*-pyrrolyl phosphines due to their strong electron withdrawing character, and the catalytic implications of this behaviour [1,2]. Evidence for the exceptional π-accepting properties of $P(pyrl)_3$ (pyrl = *N*-pyrrolyl) is provided, for example, by the complete substitution of CO in the electron-rich anion $[Rh(CO)_4]^-$ to give $[Rh\{P(pyrl)_3\}_4]^-$ [3]. Nevertheless, only a few examples of coordination compounds of transition metals stabilized with $P(pyrl)_3$ are known [1,4]. In particular, the only palladium example described so far has been obtained in our group by making the dinuclear σ/π palladium compound $[Pd(\mu\text{-}Cl)(\kappa,\eta^2\text{-}COE\text{-}MeO)]_2$ react with $P(pyrl)_3$ (Eq. (1)) [5].

* Corresponding author.
E-mail address: miquel.seco@qi.ub.es (M. Seco).

0022-328X/$ - see front matter © 2007 Elsevier B.V. All rights reserved.
doi:10.1016/j.jorganchem.2007.05.038

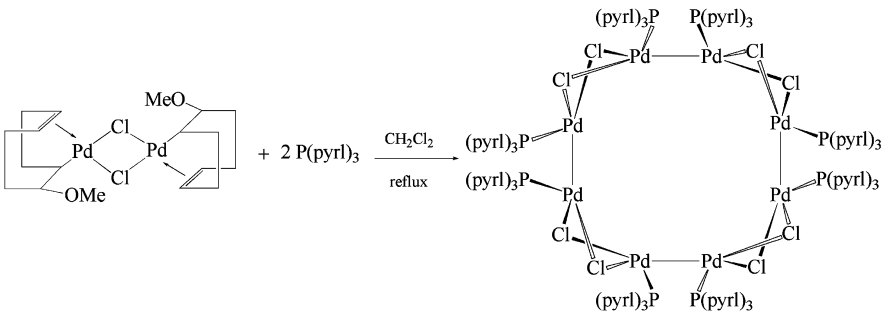

1 (1)

The molecular structure of **1** consists of an eight-palladium(I) crown-cycle containing unsupported Pd–Pd bonds. This unprecedented geometry prompted us to analyse the process carefully in order to obtain mechanistic information about its formation and this work is reported in the present paper. In this context, the reaction of $P(pyrl)_3$ with the related platinum complex, $[Pt(\mu\text{-}Cl)(\kappa,\eta^2\text{-}COE\text{-}MeO)]_2$, has proved crucial for understanding the formation of **1**. In addition, we have explored the reaction of the octapalladium cluster **1** with the chelating agent 2-[(pyridin-2-ylmethylene)aminophenol] (HNN′O), which is known to act also as a tridentate ligand [6], in an attempt to build new supramolecular structures. The resulting compound displayed an unusual $P(O)(pyrl)_2$ ligand. Finally, we describe, for the first time, the insertion of a $P(pyrl)_2$ moiety into the Pd–O bond of $[PdCl(\kappa^3\text{-}NN'O)]$, to form a six-membered palladacycle, whose structure has been revealed by X-ray crystallography.

2. Results and discussion

2.1. Palladium and platinum compounds containing P(pyrl)3

Our first goal in this paper was to investigate whether the platinum complex $[Pt(\mu\text{-}Cl)(\kappa,\eta^2\text{-}COE\text{-}MeO)]_2$ (**2**) reacts with $P(pyrl)_3$ like the analogous palladium compound does. To this end, we first prepared **2** as a white crystalline powder by reaction of NaMeO with $[PtCl_2(COD)]$ in methanol at room temperature. The ^1H, ^{13}C NMR and IR spectra confirmed the nature of the product. Next, **2** was reacted with two equivalents of $P(pyrl)_3$ in acetone at −10 °C (Eq. (2)). The process was monitored by ^{31}P NMR spectroscopy. The reaction was very clean and the ^{31}P NMR signal at 78.8 ppm due to free $P(pyrl)_3$ completely disappeared and a new resonance emerged at 68.6 ppm corresponding to the new compound **3**. After 3 h of stirring the volume of the solution was reduced and a crystalline solid precipitated by addition of hexane.

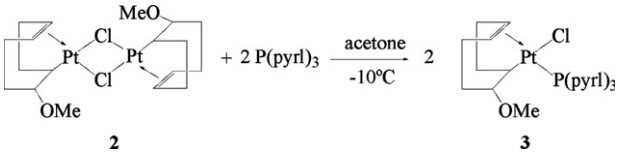

2 3 (2)

The white colour of **3** revealed that no compound, analogous to the palladium crown-cycle, had been obtained, given that the vast majority of platinum compounds containing metal–metal bonds are strongly coloured. Elemental analyses, NMR spectroscopy and MS MALDI-TOF spectrometry confirmed this hypothesis showing that **3** is the mononuclear species depicted in Eq. (2). Its formation is easily explained in terms of the rupture of the Pt–Cl bridging bonds of the dinuclear complex by the incoming phosphine. The IR spectrum of **3** showed a strong band at 1184 cm^{-1}, assigned to $\nu_{C=C}$ ring breathing pyrrole, confirming the presence of the $P(pyrl)_3$ ligand. In the ^1H NMR spectrum, the pyrrolyl protons were visible as multiplet resonances at 6.43 and 7.08 ppm. These chemical shifts appeared at slightly lower field values than those recorded for the free $P(pyrl)_3$ (6.35 and 6.78 ppm). The signals of the COE-MeO group did not undergo significant shifting from those observed in the starting complex **2**. The ^{13}C NMR spectrum of **3** showed two resonances of the $P(pyrl)_3$ carbon atoms: a doublet at 113.9 ppm ($^3J_{CP} = 8.4$ Hz) and a second doublet at 124.8 ppm ($^2J_{CP} = 8.2$ Hz). The most striking feature in the ^{31}P NMR spectrum is the signal at 68.6 ppm flanked by ^{195}Pt satellites with a J_{PPt} constant of 6546 Hz. In general, Pt(II) complexes containing functionalized *N*-pyrrolyl phosphines present J_{PPt} values in the range 3800–4800 Hz, although there are some derivatives with other phosphine ligands that show higher values, examples being $[PtCl_2\{P(pyrl)_2(N\text{-}C_7H_5N)\}_2]$ ($J_{PPt} = 5409$ Hz) [1e] and $[PtCl_2\{PF_2(NMe_2)\}_2]$ ($J_{PPt} = 5690$ Hz) [7]. The large P–Pt coupling constant of 6546 Hz is the highest reported so far for a Pt(II) complex, suggesting that the phosphine and the double carbon–carbon bond are both in *trans*. Complete assignation of signals in the NMR spectra has been achieved by NOESY ^1H–^1H, COSY ^1H–^1H and HSCQ ^1H–^{13}C experiments (see Supplementary material).

Compound **3** is rather unstable in solution, precluding the grow of single crystals for an X-ray crystal structure determination. The rate of decomposition is increased by addition of an excess of phosphine. One of the decomposition products was the complex *cis*-$[PtCl_2\{P(pyrl)_3\}_2]$ (**4**). As **4** had not been previously described we synthesized it following the classical procedure involving the reaction of $[PtCl_2(COD)]$ with $P(pyrl)_3$ in CH_2Cl_2 at room temperature. Compound **4** was characterized by elemental analyses

IR and NMR spectroscopy. Note that in this complex the J_{PPt} constant is 4801 Hz.

The formation of **3** from **2** and $P(pyrl)_3$ shed light on the hypothetical mechanism underlying the formation of **1**. It is clear that the great difference in both reactions is that the platinum derivative **2** resists the COE-MeO displacement by the phosphine, while the related palladium complex $[Pd(\mu\text{-}Cl)(\kappa,\eta^2\text{-}COE\text{-}MeO)]_2$ does not. Evidently, the ease of the COE-MeO labilization depends on the bonding energy of the metal–carbon bond, it being known that this is stronger for the platinum–carbon bond. For this reason, in the process involving the platinum complex **2** and $P(pyrl)_3$ we only observed cleavage of the platinum–chloride bond to yield **3**. However, in the case of the palladium complex, the $P(pyrl)_3$ prefers to displace the COE-MeO ligand, with the central Pd_2Cl_2 system remaining unaltered. Under these conditions, the intermediate species that now contain the one-electron σ-COE-MeO ligand was formed. This species could then undergo the homolytic rupture of the M–C bond, followed by the formation of four Pd–Pd bonds to give the cyclo-octanuclear palladium(I) complex **1** (Scheme 1). This behaviour is supported by the observation of a signal in the ESI mass spectrum of the reaction solution at $m/z = 279$ assigned to the $[(COE\text{-}MeO)_2H]^+$ species.

According to this hypothesis, supramolecular structures containing a different number of $\{pyrl\}_3PPd\text{–}PdP\{pyrl\}_3$ units, for example three or six, cannot be ruled out, although we have not been able to detect them. It is likely, as observed for simple supramolecules [8], that the square molecular species is the one preferred from a thermodynamic point of view. Finally, the question arises as to the effect that the addition of an excess of $P(pyrl)_3$ produces on **1**. In fact, solutions of **1** rapidly turned orange from red to yield $[PdCl_2(P(pyrl)_3)_2]$, which appeared impure with metallic palladium. This result is explained by assuming that **1** underwent the rupture of the Pd–Cl bridging bonds, giving unstable Pd(I) complexes which are known to show disproportionation to metal palladium and Pd(II) complexes. In other words, the complex $[PdCl(\kappa,\eta^2\text{-}COE\text{-}MeO)]_2$ firstly reacts with $P(pyr)_3$ to give **1** and then, only after the addition of an excess of phosphine, undergoes cleavage of the Pd–Cl bridging bonds. This behaviour contrasts with that observed for the platinum complex. In summary, we conclude that the formation of the octacyclopalladium cluster **1** is due to the higher lability of the coordinated C–C double bond compared with that of the Pd–Cl bonds in $[Pd(\mu\text{-}Cl)(\kappa,\eta^2\text{-}COE\text{-}MeO)]_2$.

2.2. Reaction of *1* with 2-[(pyridin-2-ylmethylene)aminophenol]

Having described above that an excess of *P*-donor ligand produces the decomposition of **1**, we became interested in studying the effect of the singular ligand *N*-donor 2-[(pyridin-2-ylmethylene)aminophenol] (HNN′O) in order to determine whether this ligand, able to act as a bis- or trischelate, could stabilize other unusual geometries. In fact, some palladium complexes containing the ligand as a bidentate or tridentate mode have recently been described [6].

Compound **1** was allowed to react with HNN′O, in the presence of NEt_3 to guarantee the anionic form of the ligand (NN′O) in CH_2Cl_2, at 0 °C. The solution rapidly turned purple and metallic palladium precipitated. After filtration, purple crystals of $[Pd(\kappa^3N,N',O\text{-}py\text{-}CH{=}N\text{-}C_6H_4O)(P(O)(pyrl)_2)]$ (**5**) could be isolated (Eq. (3)). Compound **5** was fully characterized spectroscopically and its structure was unambiguously confirmed by a single X-ray crystal structure determination.

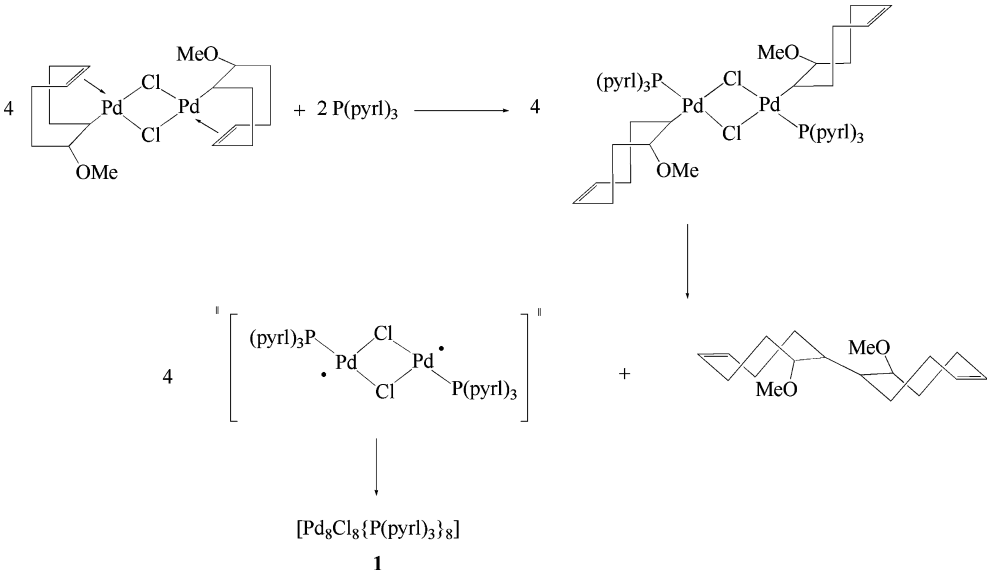

Scheme 1.

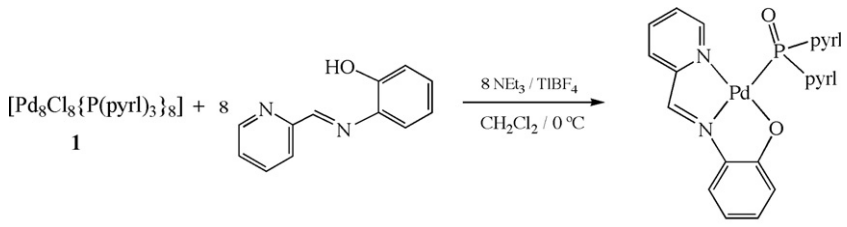

(3)

The ^{1}H NMR spectrum revealed the protons that correspond to the iminic group (8.38 ppm) and to the HC_{α}-pyridine ligand (8.25 ppm). The signal at 7.30 ppm due to the OH group of the free ligand was not observed. The ^{31}P NMR spectrum showed one signal at 41.4 ppm, far from the expected value for coordinated $P(pyrl)_3$ (in the region of about 90 ppm) and thus suggesting a significant modification on the phosphine ligand. The X-ray structure revealed that the ligand is actually the di(*N*-pyrrolyl)phosphonato-*P* group, $-P(O)(pyrl)_2$. The IR spectrum of **5** showed a sharp band at 1186 cm^{-1} assignable to the P=O stretch and the mass spectrum (MALDI-TOF) showed a signal at *m*/*z* 483 $[M]^{+}$ confirming the nature of the product. This is the first time that the $-P(O)(pyrl)_2$ group appears to be bonded to a metal centre as part of a coordination compound. The phosphine oxidation is believed to originate from adventitious water, similar to that reported in the formation of some diphosphoxane–rhodium complexes [9]. Since the process described here supposes the cleavage of Pd–Cl bonds, we repeated the reaction in the presence of $TlBF_4$, as a halide abstractor and, under these conditions, the reaction proceeded much more rapidly. In addition, the absence of chloride ligands in **5**, as well as the precipitation of palladium metal, suggests that the first step of this process would involve the displacement of the chloride from **1** by the NN′O ligand, followed by rupture of the metal–metal bond to show finally disproportionation of Pd(I) to Pd(II) and Pd(0). In conclusion, treatment of **1** with HNN′O in basic medium leads to the decomposition of the Pd_8 crown-cycle structure to yield mononuclear square planar palladium(II) complexes, in which three coordination sites are occupied by the trischelate ligand and the fourth by the di(*N*-pyrrolyl)phosphonato-*P* group.

2.3. Crystal structure of 5

The molecular structure of compound **5** was solved by X-ray crystal diffraction methods. Compound **5** crystallizes with dichloromethane. Thus, in the asymmetric unit of the unit cell a molecule of compound **5** and half molecule of dichloromethane are present. Fig. 1 shows the molecular structure of this compound and in Table 1 a selection of bond distances and angles are listed. The metal centre has a distorted square-planar coordination geometry, with the ligand behaving as NN′O-tridentate, and with the

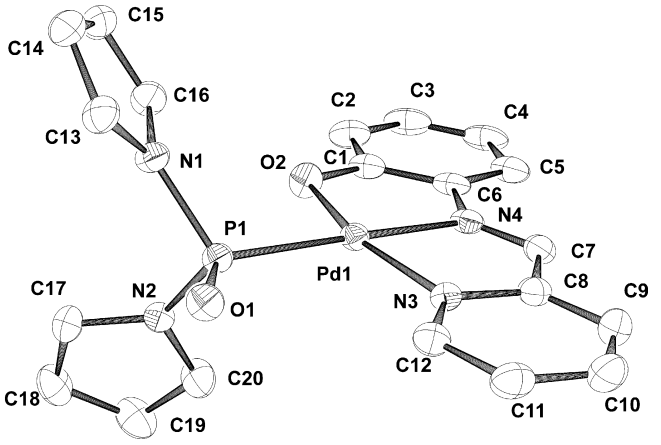

Fig. 1. Molecular structure of **5**.

Table 1
Selected bond length (Å) and selected bond angles (°) of [Pd(κ^3*N*,*N*′,*O*-py-CH=N-C_6H_4O)(P(O)(pyrl)$_2$)] (**5**) and [PdCl{κ^3*P*,*N*,*N*-(P(pyrl)$_2$-O-C_6H_4-N-CH(CH_2-CO-CH_3)-py)}] (**7**)

5		**7**	
Bond lengths (Å)			
Pd1–P1	2.2478(7)	Pd–Cl	2.3033(7)
Pd1–O2	2.0278(19)	Pd–N2	2.084(2)
Pd1–N4	2.013(2)	Pd–N1	2.0178(18)
Pd1–N3	2.056(2)	Pd–P	2.1701(7)
O2–C1	1.334(3)	C11–C7	1.502(4)
N4–C6	1.404(3)	C7–N1	1.476(3)
N4–C7	1.284(4)	N1–C6	1.387(3)
C7–C8	1.457(4)	C1–O1	1.404(3)
C8–N3	1.371(3)	P–O1	1.5963(18)
C1–C6	1.415(4)	C7–C8	1.538(4)
P1–O1	1.4862(19)	C8–C9	1.510(4)
P1–N1	1.721(2)	C9–C10	1.477(5)
P1–N2	1.719(2)	C9–O2	1.201(4)
Bond angles (°)			
P1–Pd1–N3	100.71(6)	Cl–Pd–P	97.01(3)
N3–Pd1–N4	80.53(9)	Cl–Pd–N2	96.23(6)
N4–Pd1–O2	82.67(8)	N2–Pd–N1	82.82(8)
O2–Pd1–P1	96.07(6)	N1–Pd–P	84.03(6)
Pd1–N3–C8	111.10(17)	Pd–N1–C7	107.31(14)
Pd1–N4–C7	115.97(18)	Pd–N1–C6	111.44(15)
Pd1–N4–C6	112.74(18)	Pd–P–O1	111.20(7)
Pd1–O2–C1	109.86(17)	N3–P–O1	103.19(11)
C6–N4–C7	131.3(2)	N4–P–O1	101.80(11)
		N3–P–N4	101.67(12)
		Pd–P–N3	121.35(9)
		Pd–P–N4	115.23(9)
		C6–N1–C7	117.8(2)

di(*N*-pyrrolyl)phosphonato-*P* group coordinated *trans* to the iminic nitrogen atom N(4).

The whole complex molecule, with the obvious exceptions of the pyrrolyl rings, is planar (maximum displacement less than 0.04 Å) and two five-membered chelate rings are formed upon coordination. The bite angles involved in the chelation are typical for these tridentate systems. Thus, for example, the N(3)–Pd(1)–N(4) and the N(4)–Pd(1)–O(2) angles appear at 80.53(9)° and 82.67(8)°, respectively. The Pd(1)–N(4) bond distance, 2.013(2) Å, is practically identical to that found in [Pd(κ^3-NN′O)(Me)] [6], suggesting strong *trans* influence of the –P(O)(pyrl)$_2$ ligand. The Pd(1)–O(2) distance, 2.0278(19) Å, is in agreement with those found in related hydrazone complexes [6] and the C(7)–N(4) distance of 1.284(4) Å is characteristic of a –C=N– iminic system. On the other hand, the palladium–di(*N*-pyrrolyl)phosphoryl bond length [Pd(1)–P(1), 2.2478(7) Å] is significantly shorter and falls towards the lower end of the wide range of Pd–PR$_3$ bond distances. In contrast, the P(1)–N(1) distance, 1.721(2) Å and P(1)–N(2) 1.719(2) Å, is rather large. The P(1)–O(1) distance is 1.4862(19) Å and corresponds to a P=O double bond. No other species with this di(*N*-pyrrolyl)phosphonato-*P* ligand has been previously described, and only three compounds with the P(O)N$_2$ group bound to a transition metal have been structurally described, although in one of them the phosphoryl oxygen [10] is also coordinated to another metal, and thus their structural parameters cannot be compared. In the other two examples, involving metals belonging to the first transition series (Fe, Co), the M–P bond lengths (3.081 and 2.265 Å respectively) [11,12] are greater than the Pd–P distance (2.2478(7) Å) found in **5**. This is consistent with the idea that for L$_n$M–PZ$_x$ systems, such as the M–P bond distance decreases (because of increased M–P back bonding), the P–Z lengths increase due to partial loss of back donation into P–Z σ* orbitals.

It is interesting to note that the crystal structure of this compound is also maintained for weak interactions due to both the dichloromethane solvent molecules and (*N*-pyrrolyl)phosphonato ligands (Fig. 2). The solvent molecules occupy a special position in a binary axis, and bridge two molecules of **5** through a hydrogen bond O(1)···C(21)–H(21) with [C(21)···O(1)] = 3.143(4) Å (angle C(21)–H(21)–O(1) = 149.4(3)°). Another weak hydrogen bond connects the O(1) of one ligand with the hydrogen atom H(11) of the neighbouring molecule ([C(11)···O(1)] = 3.288(3) Å and C(11)–H(11)–O(1) = 136.25(2)°).

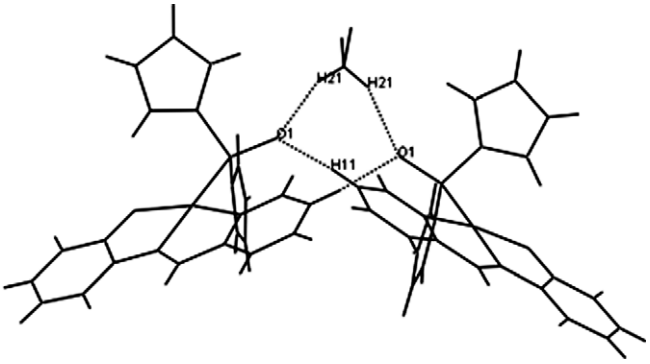

Fig. 2. Intermolecular hydrogenbonds in **5**.

2.4. Reaction of [PdCl(κ^3-NN′O)] with P(pyrl)$_3$

Having shown that the P(pyrl)$_3$ displaces the double C=C bond more easily than the bridging chloride in [Pd(μ-Cl)(κ,η^2-COE-MeO)]$_2$, we were interested to determine the behaviour of those derivatives containing simultaneously two or more sites potentially vulnerable to attack by the P(pyrl)$_3$. For this purpose, the complex [PdCl(κ^3-NN′O)] (**6**), having simultaneously Pd–Cl, Pd–N and Pd–O bonds, was thought to be a good target. Given that **6** had only been described in solution [6], we improved its synthesis by making [PdCl$_2$(COD)] react with NN′OH in THF to give [PdCl$_2$(κ^2-NN′OH)] (see Section 4). After treatment with *n*-BuLi in THF, a deep blue solution was obtained, from which purple crystals of **6** were isolated. The nature of **6** was determined by NMR spectroscopy and elemental analyses. The ^{1}H NMR spectrum of **6** showed a signal at 8.34 ppm due to α-*H*C pyridine protons, which was shifted at high fields with respect to that observed in the κ^2-NN′ coordinated species. The iminic proton also shifted from 8.70 to 8.44 ppm. Moreover, the complete disappearance of the OH group confirmed the three coordination mode for the NN′O ligand.

When a solution of **6** in acetone was treated with P(pyrl)$_3$ a dramatic change in colour was observed and, after 12 h of stirring, a deep red solution was obtained. The work-up rendered the unexpected complex [PdCl{κ^3*P*,*N*,*N*-(P(pyrl)$_2$-O-C$_6$H$_4$-N-CH(CH$_2$-CO-CH$_3$)-py)}] (**7**), (Eq. (4)), which was identified spectroscopically and by X-ray structure determination.

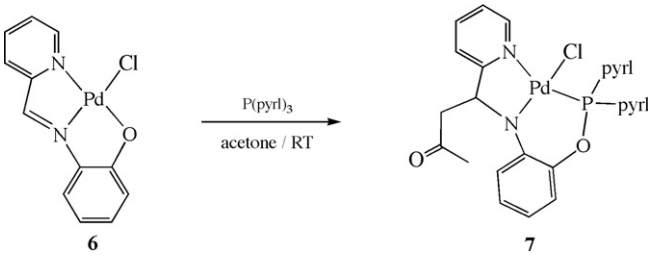

6 **7**

(4)

The ^{31}P NMR spectrum indicated the existence of one signal for the phosphorus nucleus at low field (δ = 111.8 ppm) in comparison with the free P(pyrl)$_3$ ligand, but far from the average values observed for Pd–P(pyrl)$_3$ complexes. Furthermore, the ^{1}H NMR spectrum showed the shifting of the iminic proton from 8.44 to 5.38 ppm, confirming the absence of a C=N double bond. The appearance of new signals at 1.94 and 3.04 ppm, assignable to the acetone group, was also observed. The IR spectrum showed bands at 1723 and 1020 cm^{-1} due to the $\nu_{C=O}$ and ν_{P-O} stretching, respectively. As revealed by the

X-ray crystal structure determination (see below) the most relevant features of **7** are the formal insertion of the $P(pyrl)_2$ moiety into the Pd–O bond, to give a six-membered cycle, and the formation of a C–C bond, through the incorporation of an acetone molecule.

The formation of **7** can be rationalized in the following terms. The first step would consist of the replacement of the chloride ligand by the phosphine. The second would involve the rupture of a pyrrolyl unit, followed by insertion of the $P(pyrl)_2$ moiety into the Pd–O bond (Scheme 2). The formation of a strong P–O bond would be the driving force of this process. In addition, the basic pyrrolyl group, which is a good leaving group, could promote the deprotonation of the acetone molecule and the attack by this species on the N=C double bond would thus yield the amido ligand displayed in **7**.

In conclusion, the formation of **7** could be the result of the preferential attack of the $P(pyrl)_3$ on the Pd–Cl against the Pd–O or Pd–N bonds.

2.5. Crystal structure of 7

The molecular structure of **7** is shown in Fig. 3 while the most relevant geometric features are listed in Table 1. The metal distorted square-planar coordination observed comprises the ligand [NN′O] modified by the formal insertion of a $P(pyrl)_2$ fragment between the oxygen atom and the metal centre. This conforms a six-membered ring containing four heteroatoms (N, P, O, Pd) and a five-membered [NN′] chelate ring containing the pyridinic group. Both N-pyridinic and P atoms are in *trans*, while the amido N(1) share the two fused rings and occupies the third coordination site. A chloride *trans* to amido N(1) completes the coordination around the metal.

The N(1)–Pd–N(2) angle of 82.82(8)° is similar to those found in some five-membered palladacycles, shaping an envelop form with the N(1) being the out-of-plane atom. It is noteworthy that the Pd–N(1) distance of 2.0178(18) Å is shorter than those reported for previously described amidopalladium complexes [13]. The C(7)–N(1) distance of 1.476(3) Å corresponds to a C–N single bond in contrast to that observed in **5** for the C=N iminic bond (1.284(4) Å). Although the C(6)–N(1)–C(7) angle is 117.8(2)°, the sum of the three angles at N(1) is 336.4°, close to a tetrahedral geometry, and this suggests that the lone pair is localized on the sp^3 nitrogen atom. This contrasts with the values found in structure **5** and in other palladium amido complexes, which show a roughly planar geometry [13]. The $P(pyrl)_2$ fragment is linked to the Pd

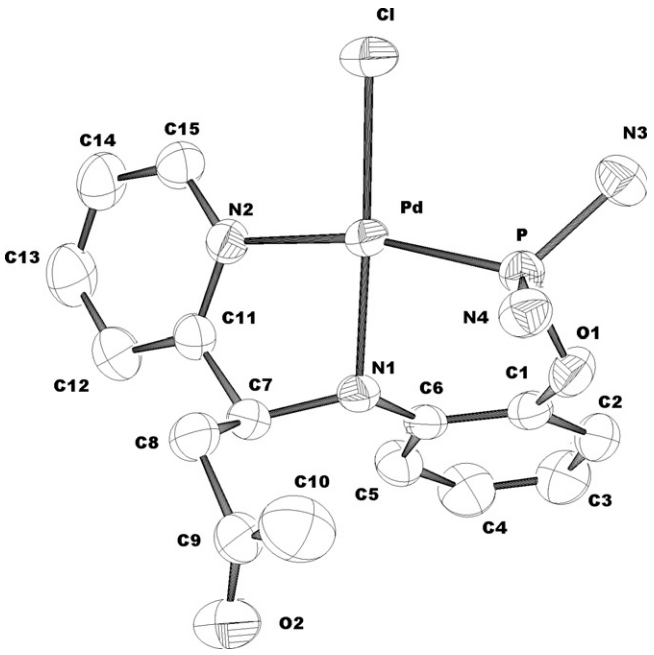

Fig. 3. Molecular structure of **7**.

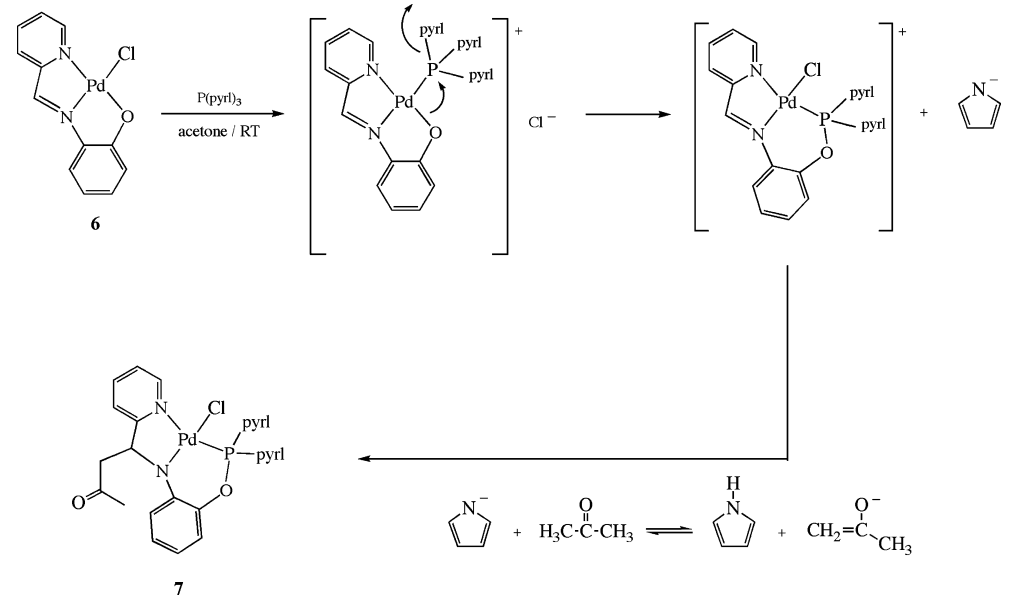

Scheme 2.

and to O(1) atoms with a P–O(1) distance of 1.5963(18) Å corresponding to a P–O single bond. The pyrrolyl groups are tilted to the oxygen atom (N(3)–P–Pd and N(4)–P–Pd angles are 121.35(9)° and 115.23(9)°, respectively) and the N(1)–C(6) distance of 1.387(3) Å is a little shorter than the average values found for N–C_{aryl} bonds. This might be due to the high strain associated with the generation of a five- and six-membered ring fused together and sharing a palladium atom with square-planar geometry. Finally, one of the most relevant features in **7** is the incorporation of an acetone molecule into the system through the C(7) iminic carbon atom.

3. Conclusion

The reaction of $[PdCl(\kappa,\eta^2\text{-COE-OMe})]_2$ with $P(pyrl)_3$ affords the eight-palladium(I) crown-cycle compound **1**, while its platinum congener **2** gives the mononuclear complex **3**, as a result of the easy cleavage of the platinum–chloride bond. The different behaviour in both cases has been ascribed to the higher lability of the C=C double bond in $[PdCl(\kappa,\eta^2\text{-COE-OMe})]_2$. Compound **1** reacts with the pyridine-aminophenol, (HNN′O), to yield the mononuclear palladium complex $[Pd(\kappa^3\text{-NN′O})(P(O)(pyrl)_2)]$ (**5**), which contains for the first time a di(*N*-pyrrolyl)phosphonato-*P* group as ligand. On the other hand, $[PdCl(\kappa^3\text{-NN′O})]$ (**6**) reacts with $P(pyrl)_3$ in acetone to give the six-membered metallacycle $[PdCl\{\kappa^3\text{-}P,N,N\text{-}(P(pyrl)_2\text{-O-}C_6H_4\text{-N-CH-}(CH_2\text{-CO-}CH_3)\text{-py})\}]$ (**7**), in which an acetone molecule has been inserted in the iminic carbon atom. The molecular structure of **7** confirms the higher lability of the Pd–Cl bond in **6** in comparison with the Pd–O or Pd–N ones.

4. Experimental

4.1. General

All reactions were carried out under an atmosphere of dry nitrogen using standard Schlenk techniques. All solvents were distilled from appropriate drying agents under N_2 prior to use. ^1H, $^{13}C\{^1H\}$, $^{31}P\{^1H\}$ and ^{195}Pt NMR spectra were recorded at 25 °C on Bruker 250 and Mercury 400 spectrometers. Chemical shifts are reported in ppm relative to external standards ($SiMe_4$ for ^1H and ^{13}C, 85% H_3PO_4 for ^{31}P) and coupling constants are given in Hz. Infrared spectra were recorded on a FT-IR 520 Nicolet spectrophotometer in the 4000–400 cm^{-1} range as KBr pellets. MS (ESI) spectra were recorded on a Fisons VG Quatro spectrometer. MALDI-TOF spectra were recorded on a Voyager DE-RP (Perspective Biosystems) time-of-flight (TOF) spectrometer.

The starting materials $[PtCl_2(COD)]_2$ [14], $[PdCl_2(COD)]_2$ [15], $P(pyrl)_3$ [3] and 2-[(pyridin-2-ylmethylene)aminophenol] (HNN′O) [6] were prepared following published procedures. Other reagents were purchased from commercial suppliers. Atom numbering in the NMR data are indicated in Scheme 3.

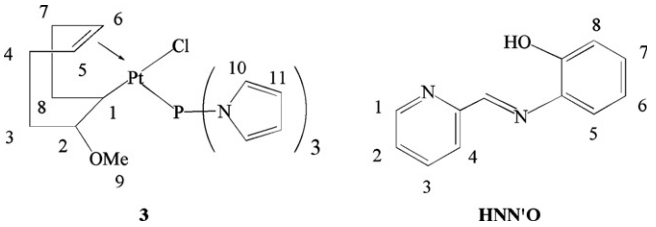

3 **HNN'O**

Scheme 3.

4.2. Synthesis of $[PtCl(\kappa,\eta^2\text{-COE-OMe})]_2$ (**2**)

A solution 0.07 M of NaOMe in methanol (23 mL, 1.61 mmol) was added to $[PtCl_2(COD)]_2$ (0.600 g, 1.60 mmol) and the mixture was stirred at room temperature for 2 h. The solvent was removed under vacuum, and the residue was re-dissolved in CH_2Cl_2 and filtered off. The solvent was evaporated to dryness and the solid washed with diethyl ether to obtain $[PtCl(\kappa,\eta^2\text{-COE-OMe})]_2$ as a colourless solid. Yield: 0.509 g, 85%. δ_H (250 MHz; $CDCl_3$): 4.73 (2H, s, $^2J_{HPt} = 76$ Hz, H_5, H_6); 3.49 (1H, m, H_2); 3.22 (3H, s, H_9); 3.0–1.0 (9H, m). δ_C (62.9 MHz; $CDCl_3$): 101.9 (s, C_5, C_6); 82.8 (s, C_2); 58.1 (s, C_9); 35.7 (s, C_3); 32.8 (s, C_4); 31.1 (s, $^1J_{CPt} = 486$ Hz, C_1); 30.0 (s, C_7); 29.7 (s, C_8). IR: ν_{max}/cm^{-1} 1087vs, 1073s (C–O). Anal. Calc. for ($C_{18}H_{30}Cl_2O_2Pt_2$): C, 29.23; H, 4.09. Found: C, 28.87; H, 2.55%.

4.3. Synthesis of $[PtCl(\kappa,\eta^2\text{-COE-OMe})(P(pyrl)_3)]$ (**3**)

A solution of $P(pyrl)_3$ (0.156 g, 0.68 mmol) in 2 mL of dichloromethane was added to a stirred solution of $[PtCl(COE\text{-}OMe)]_2$ (0.250 g, 0.34 mmol) in 20 mL of cool acetone (−10 °C). The mixture was stirred for a further 2 h at −10 °C and the resulting yellowish solution was evaporated to dryness. The residue was re-crystallized in acetone/*n*-hexane. The desired product was isolated as a colourless solid by filtration, washed with *n*-hexane and dried under vacuum. Yield: 0.324 g, 80%. δ_P (101 MHz; CD_2Cl_2): 68.6 ppm ($^1J_{PPt} = 6546$ Hz). δ_H (400 MHz; CD_2Cl_2): 7.08 (6H, m, H_{10}); 6.54 (2H, m, H_5, H_6); 6.43 (6H, m, H_{11}); 3.13 (1H, m, H_2); 2.88 (4H, m, H_8, H_9); 2.64 (1H, m, H_8); 2.31 (2H, m, H_4); 2.09 (1H, m, H_3); 1.99 (3H, m, H_7, H_3); 1.75 (1H, m, H_1). δ_C (100 MHz; CD_2Cl_2): 124.8 (d, $^2J_{CP} = 8.2$ Hz, C_{10}); 120.3 (d, $^2J_{CP} = 13.8$ Hz, $^1J_{CPt} = 81$ Hz, $C_{5\ or6}$); 119.4 (d, $^2J_{CP} = 17.3$ Hz, $^1J_{CPt} = 79$ Hz, $C_{5\ or\ 6}$); 113.9 (d, $^3J_{CP} = 8.4$ Hz, C_{11}); 82.9 (s, C_2); 56.1 (s, C_9); 35.2 (s, C_3); 31.3 (s, $^1J_{CPt} = 601$ Hz, C_1); 29.9 (s_{br}, C_7, C_8); 26.8 (s, C_4). MS (MALDI DTH-THF): *m/z* 566.3 $[M-OMe]^+$, 563.3 $[M-Cl]^+$. IR: ν_{max}/cm^{-1} 3126w (CH), 2966–2818w (CH), 1468m (C=C), 1184s (C–N), 1091–1058s (P–N–C), 742s (CH). Anal. Calc. for ($C_{21}H_{27}ClN_3OPPt$): C, 42.11; H, 4.54; N, 7.01. Found: C, 42.04; H, 4.45; N, 6.87%. ^1H–^{13}C HSQC, ^1H–^1H COSY, ^1H–^1H NOESY: see supporting data in Supplementary material.

4.4. Synthesis of $[PtCl_2\{P(pyrl)_3\}_2]$ (4)

To a stirred solution of $P(pyrl)_3$ (0.260 g, 1.13 mmol) in 10 mL of dichloromethane at room temperature was added $[PtCl_2(COD)]$ (0.207 g, 0.55 mmol). The solution was stirred for 30 min and the addition of *n*-hexane gave the desired product. Compound **4** was isolated by filtration as a colourless powder. Yield: 0.270 g, 67%. δ_P (101 MHz; $CDCl_3$): 51.4 ($^1J_{PPt} = 4801$ Hz). δ_H (250 MHz; $CDCl_3$): 6.81 (12H, m), 6.28 (12H, m). δ_C (62.9 MHz; $CDCl_3$): 124.8 (t, $^2J_{CP} = 4.1$ Hz), 114.6 (t, $^3J_{CP} = 4.7$ Hz). δ_{Pt} (53.8 MHz; $CDCl_3$): −4258.7 (t, $^1J_{PPt} = 4800$ Hz). IR: ν_{max}/cm^{-1} 3137w (CH), 1457m (C=C), 1184vs (C–N), 1069vs (P–N–C), 726vs (CH). Anal. Calc. for ($C_{24}H_{24}Cl_2N_6P_2Pt$): C, 39.79; H, 3.34; N, 11.59. Found C, 39.83; H, 3.40; N, 11.37%.

4.5. Synthesis of $[Pd(\kappa^3\text{-}NN'O)(P(O)(pyrl)_2)]$ (5)

A solution of **1** (0.063 g, 0.212 mmol) in 15 mL of CH_2Cl_2 was added to a solution of HNN′O (0.051 g, 0.257 mmol) and NEt_3 (6 mL, 43 mmol) in 15 mL of CH_2Cl_2 at 0 °C. The mixture was stirred for 1 h, and $TlBF_4$ (0.050 g, 0.626 mmol) was added. The solution that resulted was filtered off and evaporated to dryness. The purple residue was washed with diethyl ether and re-crystallized in CH_2Cl_2/hexane to obtain **5** as a purple solid. Yield: 0.025 g, 60%. δ_P (101 MHz; $CDCl_3$): 41.4. δ_H (250 MHz; $CDCl_3$): 8.38 (s, CH=N), 8.25 (d, H_1), 8.20–6.5 (m, H_{2-8}), 7.33 (m, pyrl), 6.27 (m, pyrl). IR: ν_{max}/cm^{-1} 3100–3033w (CH), 1581m (C=N), 1488, 1454m (C=C), 1186s (P=O), 1078–1038s (P–N–C), 754s (CH). MS (MALDI DTH-THF): *m/z* 483.3 $[M]^+$. Anal. Calc. for ($C_{20}H_{17}N_4O_2PPd$): C, 49.76; H, 3.55; N, 11.60. Found C, 49.83; H, 3.40; N, 11.47%.

4.6. Synthesis of $[PdCl_2(\kappa^2\text{-}NN'OH)]$

To a stirred solution of $[PdCl_2(COD)]$ (0.040 g, 0.14 mmol) in 50 mL of tetrahydrofuran at room temperature was added the ligand HNN′O (0.028 g, 0.14 mmol) and the mixture was stirred for 2 h. The brown solid obtained was filtered off and dried under vacuum. Yield: 0.050 g, 95%. δ_H (250 MHz; DMSO-d_6): 10.03 (1H, br s, OH); 9.04 (1H, d, $J = 5.6$ Hz, H_1); 8.70 (1H, s, CH=N); 8.38 (1H, t, $J = 7.7$ Hz, H_3); 8.18 (1H, d, $J = 7.6$ Hz, H_4); 7.93 (1H, d, $J \approx 6.8$ Hz, H_2); 7.15 (2H, m, H_5, H_6); 6.89 (1H, d, $J = 8.5$ Hz, H_8); 6.81 (1H, t, $J = 7.6$ Hz, H_7). IR: ν_{max}/cm^{-1} 3262vs (O–H), 3050w (CH), 1594m (C=N), 1505, 1456m (C=C), 764s (CH).

4.7. Synthesis of $[PdCl(\kappa^3\text{-}NN'O)]$ (6)

To a solution of compound $[PdCl_2(\eta^2\text{-}NN'OH)]$ (0.147 g, 0.39 mmol) in 30 mL of tetrahydrofuran was added 250 μL of *n*-BuLi 1.6 M (0.40 mmol) and the mixture was stirred 1 h at room temperature. The purple solid obtained was filtered off and dried under vacuum. Yield: 0.090 g, 68%. δ_H (250 MHz; DMSO-d_6): 8.44 (1H, br s, CH=N); 8.34 (1H, d, $J = 4.4$ Hz, H_1); 8.13 (1H, t, $J = 7.5$ Hz, H_3); 7.75 (1H, d, $J \approx 7.5$ Hz, H_4); 7.59 (1H, m, H_2); 7.37 (1H, d, $J = 7.9$ Hz, H_5); 7.03 (1H, t, $J \approx 7.2$ Hz, H_6); 6.45 (2H, m, H_7, H_8). IR: ν_{max}/cm^{-1} 3020w (CH), 1589m (C=N), 1475, 1451m (C=C), 740s (CH). Anal. Calc. for ($C_{12}H_9ClN_2OPd$): C, 42.51; H, 2.67; N, 8.25. Found: C, 42.59; H, 2.60; N, 8.09%.

4.8. Synthesis of $[PdCl\{\kappa^3\text{-}P,N,N\text{-}(P(pyrl)_2\text{-}O\text{-}C_6H_4\text{-}N\text{=}CH(CH_2\text{–}CO\text{–}CH_3)\text{-}py)\}]$ (7)

A solution of $P(pyrl)_3$ (0.036 g, 0.16 mmol) in 2 mL of acetone was added to a solution of compound $[PdCl(\eta^3\text{-}NN'O)]$ (0.053 g, 0.16 mmol) in 10 mL of the same solvent and the mixture was stirred over night. The solvent was evaporated to dryness and the crude was extracted 3 times with 15 mL of diethyl ether. Removal of the solvent followed by drying under vacuum gave **7** as a red solid. Yield: 0.038 g, 43%. Crystals suitable for X-ray analyses were obtained by slow diffusion of *n*-hexane in a CH_2Cl_2 solution of compound **7**. δ_P (101 MHz; $CDCl_3$): 111.8. δ_H (250 MHz; $CDCl_3$): 8.95 (1H, m, H_1); 7.87 (1H, t, H_3); 7.56 (1H, d, H_2); 7.36 (3H, br s, H_4, pyrl); 7.14 (2H, m, pyrl); 6.98 (2H, m, H_5, H_6); 6.83 (1H, d, H_8); 6.65 (1H, t, H_7); 6.47 (2H, m, pyrl); 6.39 (2H, m, pyrl); 5.38 (1H, m, CHN); 3.04 (2H, m, CH_2); 1.94 (3H, s, CH_3). IR ν_{max}/cm^{-1}: 3120 w (CH), 2966m (CH), 1723m (C=O), 1602m (C=N), 1481, 1461m (C=C), 1259s (C–N), 1065vs (P–N–C), 1020m (P–O), 803s (CH). MS ESI(+): $m/z = 523.0$ $[M-Cl]^+$. Anal. Calc. for ($C_{23}H_{22}ClN_4O_2PPd$): C, 49.39; H, 3.96; N, 10.11. Found C, 49.20; H, 3.87; N, 9.82%.

4.9. X-ray structure determination of 5

Crystallographic and experimental details of the crystal structure determinations are given in Table 2. A suitable crystal of complex **5** was covered with mineral oil and mounted in the N_2 stream of a Bruker-Nonius Kappa CCD diffractometer and data were collected using graphite-monochromated Mo Kα radiation ($\lambda = 0.71073$ Å). Data collections were performed at low temperature 150 K with an exposure time of 6 s per frame (13 sets; 1274 frames). Raw data were corrected for Lorenz and polarization effects. The structure was solved by direct methods, completed by the subsequent difference Fourier techniques and refined by full-matrix least-squares on F^2 (SHELXL-97) [16]. Anisotropic thermal parameters were used in the last cycles of refinement for the non-hydrogen atoms. The hydrogen atoms were included from geometrical calculations and refined using a riding model. All the calculations were made using the WinGX system [17].

4.10. X-ray structure determination of 7

A prismatic crystal of **7** was selected and mounted on a MAR345 diffractometer with image plate detector.

Table 2
Crystal data and structure refinement for **5** and **7**

Compound	**5**	**7**
Empirical formula	$C_{20}H_{17}ClN_4O_2PPd \cdot 0.5CH_2Cl_2$	$C_{23}H_{22}ClN_4O_2PPd$
Formula weight (g/mol)	525.21	559.27
Colour	Purple	Red
Crystal size (mm)	$0.3 \times 0.28 \times 0.2$	$0.1 \times 0.1 \times 0.2$
Crystal system	Monoclinic	Orthorhombic
Space group	*C*12/*c*1	*Pbca*
V (Å^3)	4105.9(9)	4620.4(6)
Z	8	8
Unit cell dimensions		
a (Å)	20.598(2)	9.0060(10)
b (Å)	8.2548(14)	17.2090(10)
c (Å)	24.1512(12)	29.8120(10)
α (°)	90	90
β (°)	90.922(12)	90
γ (°)	90	90
Index ranges	$-26 \leqslant h \leqslant 26$, $-10 \leqslant k \leqslant 10$, $-31 \leqslant l \leqslant 31$	$0 \leqslant h \leqslant 12$, $0 \leqslant k \leqslant 25$, $0 \leqslant l \leqslant 43$
Radiation type	Mo Kα	Mo Kα
D_{calc} (Mg/m^3)	1.699	1.608
μ (mm^{-1})	1.138	1.016
θ Range (°)	3.14–27.51	2.46–31.61
λ (Å)	0.71073	0.71073
F(000)	2104	2256
T (K)	150(2)	293(2)
Goodness-of-fit	1.048	1.242
Data collected	62 592	44 591
Unique observed data [$I > 2\sigma(I)$] (R_{int})	4720 (0.1231)	7281 (0.0390)
Absorption correction	None	None
Parameters refined	271	293
Final R indices [$I > 2\sigma(I)$]	$R_1 = 0.0313$, $wR_2 = 0.0755$	$R_1 = 0.0458$, $wR_2 = 0.0885$
R indices (all data)[a]	$R_1 = 0.0400$, $wR_2 = 0.0796$	$R_1 = 0.0499$, $wR_2 = 0.0899$

[a] $R_1 = \sum\|F_o| - |F_c\|/[\sum|F_o|]$; $wR_2 = \{[\sum w(F_o^2 - F_c^2)^2]/[\sum w(F_o^2)^2]\}^{1/2}$.

Crystallographic and experimental details are summarized in Table 2. Unit-cell parameters were determined from 32 825 reflections ($3° < \theta < 31°$) and refined by least-squares method. Intensities were collected with graphite-monochromatized Mo Kα radiation. 44 591 reflections were measured in the range $2.46° \leqslant \theta \leqslant 31.61°$. 7281 of which were non-equivalent by symmetry (R (on I) = 0.039). 6900 reflections were assumed as observed applying the condition $I > 2\sigma(I)$. Lorentz-polarization but no absorption corrections were made. The structure was solved by direct methods, using the SHELXS computer program and refined by full-matrix least-squares method with the SHELX-97 computer program [16].

Acknowledgements

We acknowledge support from the Ministerio de Ciencia y Tecnología (Project BQU2003-01131) and the CIRIT (Generalitat de Catalunya) (Project 2001SGR 00054). I.A. is indebted to the Ministerio de Ciencia y Tecnologia for a scholarship.

Appendix A. Supplementary material

CCDC 629341 and 628858 contain the supplementary crystallographic data for **5** and **7**. These data can be obtained free of charge via http://www.ccdc.cam.ac.uk/conts/retrieving.html, or from the Cambridge Crystallographic Data Centre, 12 Union Road, Cambridge CB2 1EZ, UK; fax: (+44) 1223-336-033; or e-mail: deposit@ccdc.cam.ac.uk. Supplementary data associated with this article can be found, in the online version, at doi:10.1016/j.jorganchem.2007.05.038.

References

[1] (a) V. Rodríguez, B. Donnadieu, S. Sabo-Etienne, B. Chaudret, Organometallics 17 (1998) 3809–3814;
(b) J. Castro, A. Moyano, M.A. Pericàs, A. Riera, M.A. Maestro, J. Mahía, Organometallics 19 (2000) 1704–1712;
(c) C.D. Andrews, A.D. Burrows, J.M. Lynam, M.F. Mahon, M.T. Palmer, New J. Chem. 25 (2001) 824–826;
(d) J. Huang, C.M. Haar, S.P. Nolan, W.J. Marshall, K.G. Moloy, J. Am. Chem. Soc. 120 (1998) 7806–7815;
(e) A.D. Burrows, M.F. Mahon, M. Varrone, Dalton Trans. (2003) 4718–4730.
[2] (a) A.M. Trzeciak, T. Glowiak, R. Grzybek, J.J. Ziólkowski, J. Chem. Soc., Dalton Trans. (1997) 1831–1837;
(b) A.M. Trzeciak, T. Glowiak, J.J. Ziólkowski, J. Organomet. Chem. 552 (1998) 159–164;
(c) A.M. Trzeciak, B. Borak, Z. Ciunik, J.J. Ziólkowski, M.F.C. Guedes da Silva, A.J.L. Pombeiro, Eur. J. Inorg. Chem. (2004) 1411–1419.
[3] K.G. Moloy, J.L. Petersen, J. Am. Chem. Soc. 117 (1995) 7696–7710.
[4] (a) C.E.F. Rickard, W.R. Roper, S.D. Woodgate, L.J. Wright, J. Organomet. Chem. 643–644 (2002) 168–173;
(b) C. Babij, C.S. Browning, D.H. Farrar, I.O. Koshevoy, I.S. Podkorytov, A.J. Poë, S.P. Tunik, J. Am. Chem. Soc. 124 (2002) 8922–8931;
(c) A.D. Burrows, R.W. Harrington, M.F. Mahon, M.T. Palmer, F. Senia, M. Varrone, Dalton Trans. (2003) 3717–3726;
(d) A.D. Burrows, M.F. Mahon, M. Varrone, Dalton Trans. (2004) 3321–3330;
(e) G.R. Clark, G.-L. Lu, C.E.F. Rickard, W.R. Roper, L.J. Wright, J. Organomet. Chem. 690 (2005) 3309–3320;
(f) R.A. Stockland Jr., M.C. Kohler, I.A. Guzei, M.E. Kastner, J.A. Bawiec III, D.C. Labaree, R.B. Hochberg, Organometallics 25 (2006) 2475–2485.
[5] I. Angurell, I. Martínez-Ruiz, O. Rossell, M. Seco, P. Gómez-Sal, A. Martín, Chem. Commun. (2004) 1712–1713.
[6] A. Bacchi, M. Carcelli, C. Pelizzi, G. Pelizzi, P. Pelagatti, S. Ugolotti, Eur. J. Inorg. Chem. (2002) 2179–2187.
[7] J. Chatt, R. Mason, D.W. Meek, J. Am. Chem. Soc. 97 (1975) 3826–3827.
[8] (a) M. Ferrer, M. Mounir, O. Rossell, E. Ruiz, M.A. Maestro, Inorg. Chem. 42 (2003) 5890–5899;
(b) M. Ferrer, L. Rodríguez, O. Rossell, J. Organomet. Chem. 681 (2003) 158–166.
[9] A.D. Burrows, M.F. Mahon, M.T. Palmer, M. Varrone, Inorg. Chem. 41 (2002) 1695–1697.
[10] H. Nakazawa, Y. Kadoi, T. Mizuta, K. Miyoshi, H. Yoneda, J. Organomet. Chem. 366 (1989) 333–342.

[11] M. Nieger, E. Niecke, R. Detsch, [BADMEZ] Cambridge Structural Database, V5.27, January 2006.
[12] A.K.-S. Tse, Ru-ji Wang, T.C.W. Mak, Kin Shing Chan, J. Chem. Soc., Chem. Commun. (1996) 173–174.
[13] (a) M. Yamashita, J.F. Hartwig, J. Am. Chem. Soc. 126 (2004) 5344–5345;
(b) M.W. Hooper, J.F. Hartwig, Organometallics 22 (2003) 3394–3403;
(c) N. Kuhn, M. Grathwohl, C. Nachtigal, M. Steimann, Z. Naturforsch. B 56 (2001) 704–710;
(d) W. Henderson, B.K. Nicholson, A.G. Oliver, Polyhedron 13 (1994) 3099–3104.
[14] J.X. McDermott, J.F. White, G.M. Whitesides, J. Am. Chem. Soc. 98 (1976) 6521–6528.
[15] J. Chatt, L.M. Vallarino, L.M. Venanzi, J. Chem. Soc. (1957) 3413–3416.
[16] G.M. Sheldrick, SHELXL-97: Program for Crystal Structure Analysis, University of Göttingen, Göttingen, Germany, 1998.
[17] WinGX System: L.J. Farrugia, J. Appl. Crystallogr. 32 (1999) 837–838.